TECHNICAL ARTICLE

Crystal structure of mupirocin form I, $C_{26}H_{44}O_9$

James A. Kaduk,[1a] Kai Zhong,[2] Amy M. Gindhart,[2] and Thomas N. Blanton[2]
[1]*Illinois Institute of Technology, 3101 S. Dearborn Street, Chicago, Illinois 60616*
[2]*ICDD, 12 Campus Blvd., Newtown Square, Pennsylvania 19073-3273*

(Received 12 December 2015; accepted 4 February 2016)

The crystal structure of mupirocin Form I has been solved and refined using synchrotron X-ray powder diffraction data, and optimized using density functional techniques. Mupirocin Form I crystallizes in space group $P2_1$ (#4) with $a = 12.562\,81(16)$, $b = 5.103\,63(4)$, $c = 21.713\,34(29)$ Å, $\beta = 100.932(1)°$, $V = 1366.91(2)$ Å^3, and $Z = 2$. Although the three hydroxyl groups and the carboxylic acid participate in a three-dimensional hydrogen bond network, the crystal energy appears to be dominated by van der Waals interactions. The Rietveld-refined and density functional optimized structures differ significantly. The powder pattern has been submitted to ICDD for inclusion in the Powder Diffraction File™. © *2016 International Centre for Diffraction Data.*
[doi:10.1017/S088571561600004X]

Key words: Bactroban, mupirocin, powder diffraction, Rietveld refinement, density functional theory

I. INTRODUCTION

Mupirocin (trade name Bactroban) is an antibiotic of the monoxycarbolic acid class, used as a topical treatment for bacterial skin infections. Pseudomonic acid produced by *Pseudomonas fluorescens* was reported in 1971 (Fuller *et al.*, 1971). Subsequent investigations revealed the pseudomonic acid is a mixture of compounds with similar structures; these compounds were named as pseudomonic acids A, B, C, and D. The term mupirocin was adopted as the approved name for the main phase pseudomonic acid A (Sutherland *et al.*, 1985). Three crystalline polymorphs of mupirocin are reported in U.S. Patent 5,594,026 (Greenway *et al.*, 1997). The systematic name (CAS Registry number 12650-69-0) is 9-[(E)-4-[(2S,3R,4R,5S)-3,4-dihydroxy-5-[[(2S,3S)-3-hydroxybutan-2-yl]oxiran-2-yl]methyl]oxan-2-yl]-3-methylbut-2-enoyl]oxynonanoic acid. A two-dimensional molecular diagram is shown in Figure 1.

The presence of high-quality reference powder patterns in the Powder Diffraction File (PDF; ICDD, 2014) is important for phase identification, particularly by pharmaceutical, forensic, and law enforcement scientists. The crystal structures of a significant fraction of the largest dollar volume pharmaceuticals have not been published, and thus calculated powder patterns are not present in the PDF-4 databases. Sometimes experimental patterns are reported, but they are generally of low quality. This structure is a result of collaboration among ICDD, Illinois Institute of Technology (IIT), Poly Crystallography Inc., and Argonne National Laboratory to measure high-quality synchrotron powder patterns of commercial pharmaceutical ingredients, include these reference patterns in the PDF, and determine the crystal structures of these active pharmaceutical ingredients (APIs).

Even when the crystal structure of an API is reported, the single-crystal structure was often determined at low temperature. Most powder measurements are performed at ambient conditions. Thermal expansion (often anisotropic) means that the peak positions calculated from a low-temperature single-crystal structure often differ significantly from those measured at ambient conditions. These peak shifts can result in failure of default search/match algorithms to identify a phase, even when it is present in the sample. High-quality reference patterns measured at ambient conditions are thus critical for easy identification of APIs using standard powder diffraction practices.

II. EXPERIMENTAL

Mupirocin was a commercial reagent, purchased from the United States Pharmacopeia (Lot G0M003), and was used as-received. The white powder was packed into a 1.5 mm diameter Kapton capillary, and rotated during the measurement at ~50 cycles s^{-1}. The powder pattern was measured at 295 K at beam line 11-BM (Lee *et al.*, 2008; Wang *et al.*, 2008) of the Advanced Photon Source at Argonne National Laboratory using a wavelength of 0.413 685 Å from 0.5° to 50°2θ with a step size of 0.001° and a counting time of 0.1 s step^{-1}. The pattern was indexed on a primitive monoclinic unit cell having $a = 12.5659$, $b = 5.1036$, $c = 21.7147$ Å, $\beta = 100.913°$, $V = 1367.42$ Å^3, and $Z = 2$ using DICVOL06 (Louër and Boultif, 2007). Even given the presence of impurity phases, one unit cell was much better than the others [M/F(28) = 45.9/690.5], so it was selected and confirmed by the solution and refinement of the structure. An analysis of systematic absences using EXPO2013 (Altomare *et al.*, 2013) suggested that the space group was $P2_1$ (#4), which was confirmed by successful solution and refinement of the structure. A reduced cell search in the Cambridge Structural Database (Allen, 2002) yielded no hits.

A mupirocin molecule was built and its conformation optimized using Spartan '14 (Wavefunction, 2013), and saved as a mol2 file. This molecule (using the 1°–20° portion of the pattern) was used to solve the structure with DASH 3.3.2

[a]Author to whom correspondence should be addressed. Electronic mail: kaduk@polycrystallography.com

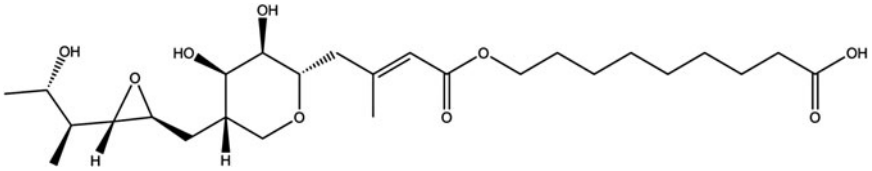

Figure 1. The molecular structure of mupirocin.

(David *et al.*, 2006). One of the 25 solutions was much better than the others. After preliminary refinement suggested that the conformation of the ring portion of the molecule was not correct, it was extracted from the crystal structure, re-optimized using Spartan '14, and saved as a new .mol2 file. Another structure solution using DASH yielded one solution which was much better than the other 24 and which was used for refinement. Ultimately, the result of the density functional theory (DFT) optimization was used as the starting model for the final refinement.

Rietveld refinement was carried out using GSAS (Larson and Von Dreele, 2004). Only the 1.5°–20.0° portion of the pattern was included in the refinement ($d_{min} = 1.19$ Å). Although there were a few, very weak peaks at higher angles, the background between 20° and 25°2θ contained a feature which was difficult to fit. Adding more terms to either the diffuse scattering or shifted Chebyshev functions caused the background to start to follow the Bragg peaks, resulting in distortion of the structure. Since the purpose of the Rietveld refinement was to provide a starting model for the DFT calculation, we judged that it was better to neglect a small number of weak peaks to obtain a more chemically reasonable structural model. All non-H bond distances and angles were subjected to restraints, based on a Mercury/Mogul Geometry Check (Bruno *et al.*, 2004; Sykes *et al.*, 2011) of the molecule. The Mogul average and standard deviation for each quantity were used as the restraint parameters. The restraints contributed 11.0% to the final χ^2. Isotropic displacement coefficients were refined and grouped by chemical similarity. The hydrogen atoms were included in calculated positions, which were recalculated during the refinement. The U_{iso} of each hydrogen atom was constrained to be 1.3× that of the heavy atom to which it is attached. The peak profiles were described using profile function #4 (Thompson *et al.*, 1987; Finger *et al.*, 1994), which includes the Stephens (1999) anisotropic strain broadening model. The background was modeled using a three-term shifted Chebyshev polynomial, with a five-term diffuse scattering function to model the Kapton capillary and any amorphous component. The final refinement of 121 variables using 18 585 observations (18 501 data points and 84 restraints) yielded the residuals $R_{wp} = 0.1152$, $R_p = 0.0844$, and $\chi^2 = 4.884$. A Le Bail fit yielded residuals $R_{wp} = 0.0788$, $R_p = 0.0648$, and $\chi^2 = 2.986$. The largest peak (1.80 Å from C31) and hole (2.08 Å from C29) in the difference Fourier map were 0.52 and −0.50 e(Å^{-3}), respectively. The Rietveld plot is included as Figure 2. The largest errors are peaks unaccounted for by this structure, and indicate the presence of a minor amount of an unidentified impurity.

A density functional geometry optimization (fixed experimental unit cell) was carried out using CRYSTAL09 (Dovesi *et al.*, 2005). The basis sets for the H, C, and O atoms were those of Gatti *et al.* (1994). The calculation used eight *k*-points and the B3LYP functional, and took ~17 days on a 3.0 GHz PC.

III. RESULTS AND DISCUSSION

The powder pattern corresponds to that of Form I of mupirocin, as described by Greenway *et al.* (1997), so the crystal structure reported here is that of Form I. The refined atom coordinates of mupirocin Form I are reported in Table I, and the coordinates from the DFT optimization in Table II. The U_{iso} of the atoms at the C1–O8 end of the

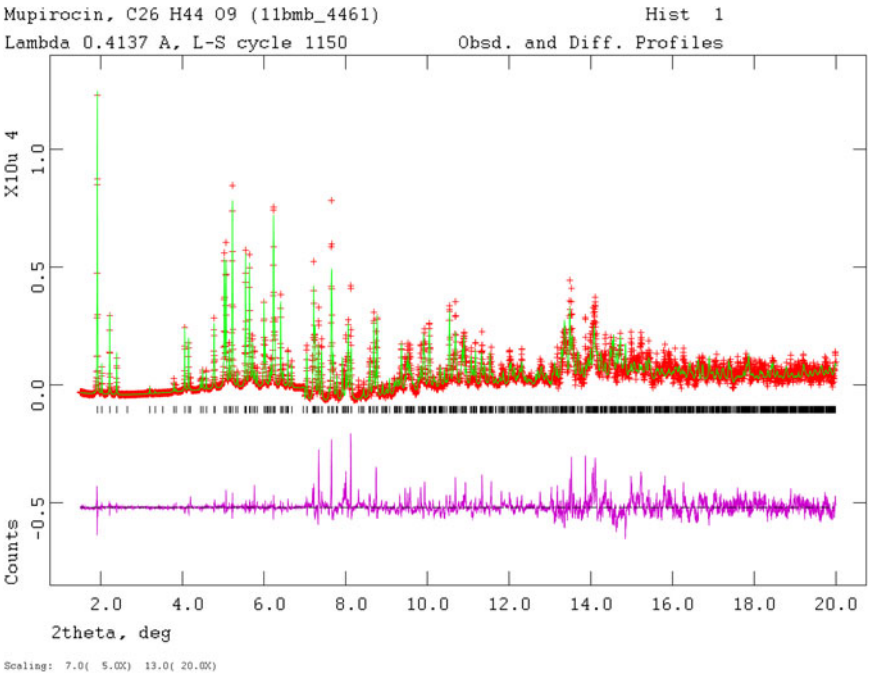

Figure 2. (Color online) The Rietveld plot for the refinement of mupirocin Form I. The red crosses represent the observed data points, and the green line is the calculated pattern. The magenta curve is the difference pattern, plotted at the same vertical scale as the other patterns. The vertical scale has been multiplied by a factor of 5 for $2\theta > 7.0°$ and by a factor of 20 for $2\theta > 17.0°$.

https://doi.org/10.1017/S088571561600004X Published online by Cambridge University Press

TABLE I. Rietveld refined crystal structure of mupirocin Form I.

Crystal data	
$C_{26}H_{44}O_9$	$\beta = 100.932\ (1)^\circ$
$M_r = 500.63$	$V = 1366.91\ (2)$ Å^3
Monoclinic, $P2_1$	$Z = 2$
$a = 12.562\ 81\ (16)$ Å	Synchrotron radiation, $\lambda = 0.413\ 685$ Å
$b = 5.103\ 63\ (4)$ Å	$T = 295$ K
$c = 21.713\ 34\ (29)$ Å	Cylinder, 1.5 × 1.5 mm
Data collection	
11-BM APS diffractometer	Scan method: step
Specimen mounting: Kapton capillary	$2\theta_{min} = 0.5^\circ$, $2\theta_{max} = 50.0^\circ$, $2\theta_{step} = 0.001^\circ$
Data collection mode: transmission	
Refinement	
Least-squares matrix: full	18 501 data points
$R_p = 0.084$	Profile function: CW Profile function number 4 with 21 terms. Pseudovoigt profile coefficients as parameterized in Thompson *et al.* (1987). Asymmetry correction of Finger *et al.* (1994). Microstrain broadening by Stephens (1999). #1(GU) = 1.163 #2(GV) = −0.126 #3(GW) = 0.063 #4(GP) = 0.000 #5 (LX) = 0.173 #6(ptec) = 0.00 #7(trns) = 0.00 #8(shft) = 0.0000 #9(sfec) = 0.00 #10(S/L) = 0.0011 #11 (H/L) = 0.0011 #12(eta) = 1.0000 #13(S400) = 5.0×10^{-2} #14(S040) = 1.6E+00 #15(S004) = 3.4×10^{-3} #16(S220) = 2.4×10^{-2} #17(S202) = -3.4×10^{-3} #18(S022) = 8.5×10^{-2} #19(S301) = 1.2×10^{-2} #20(S103) = -2.6×10^{-4} #21(S121) = -9.7×10^{-3} Peak tails are ignored where the intensity is below 0.0010 times the peak Aniso. broadening axis 0.0 0.0 1.0
$R_{wp} = 0.115$	121 parameters
$R_{exp} = 0.055$	84 restraints
$R(F^2) = 0.142\ 33$	$(\Delta/\sigma)_{max} = 0.03$
$\chi^2 = 4.884$	Background function: GSAS Background function number 1 with 3 terms. Shifted Chebyshev function of 1st kind 1: 311.342 2: −238.253 3: 96.2915

Fractional atomic coordinates and isotropic displacement parameters (Å^2)

	x	y	z	U_{iso}
C1	0.1652 (13)	0.230 41	0.5888 (10)	0.8
C2	0.2722 (12)	0.276 (4)	0.6355 (6)	0.8
O3	0.2621 (16)	0.502 (5)	0.6752 (8)	0.8
C4	0.3714 (8)	0.307 (5)	0.6047 (6)	0.8
C5	0.4142 (15)	0.589 (5)	0.6092 (11)	0.8
C6	0.3459 (11)	0.219 (4)	0.5362 (5)	0.8
C7	0.2985 (8)	0.392 (4)	0.4850 (5)	0.8
O8	0.4130 (7)	0.324 (7)	0.4947 (7)	0.8
C9	0.2272 (9)	0.296 (3)	0.4247 (5)	0.235 (3)
C10	0.1519 (8)	0.510 (3)	0.3903 (4)	0.235 (3)
C11	0.1995 (5)	0.761 (3)	0.3710 (4)	0.235 (3)
O12	0.1271 (6)	0.878 (4)	0.3206 (4)	0.235 (3)
C13	0.0280 (6)	0.962 (3)	0.3384 (4)	0.235 (3)
C14	−0.0229 (6)	0.773 (4)	0.3822 (3)	0.235 (3)
C15	0.0550 (6)	0.577 (3)	0.4207 (4)	0.235 (3)
O16	−0.0710 (10)	0.920 (3)	0.4254 (5)	0.235 (3)
O17	0.0895 (9)	0.676 (3)	0.4821 (4)	0.235 (3)
C18	−0.0497 (7)	1.024 (3)	0.2761 (4)	0.0671 (19)
C19	−0.0283 (7)	0.857 (3)	0.2215 (4)	0.0671 (19)
C20	−0.0811 (9)	0.590 (4)	0.2167 (6)	0.0671 (19)
C21	0.0183 (8)	0.938 (3)	0.1743 (4)	0.0671 (19)
C22	−0.0026 (6)	0.808 (3)	0.1122 (4)	0.0671 (19)
O23	−0.0738 (6)	0.645 (3)	0.0968 (4)	0.0671 (19)
O24	0.0807 (6)	0.831 (3)	0.0828 (4)	0.0671 (19)
C25	0.0958 (7)	0.624 (3)	0.0387 (5)	0.0363 (9)
C26	0.2135 (7)	0.594 (4)	0.0304 (5)	0.0363 (9)
C27	0.2442 (8)	0.554 (4)	−0.0412 (6)	0.0363 (9)
C28	0.3548 (9)	0.717 (4)	−0.0611 (5)	0.0363 (9)
C29	0.3981 (9)	0.624 (4)	−0.1136 (5)	0.0363 (9)
C30	0.5181 (8)	0.702 (4)	−0.1120 (5)	0.0363 (9)
C31	0.5550 (8)	0.609 (4)	−0.1653 (4)	0.0363 (9)
C32	0.6695 (7)	0.693 (4)	−0.1690 (4)	0.0363 (9)
C33	0.6933 (7)	0.787 (3)	−0.2324 (4)	0.0363 (9)
O34	0.7085 (6)	1.026 (3)	−0.2432 (4)	0.0363 (9)

Continued

https://doi.org/10.1017/S088571561600004X Published online by Cambridge University Press

TABLE I. Continued

	x	y	z	U_{iso}
O35	0.7375 (6)	0.610 (3)	−0.2585 (4)	0.0363 (9)
H36	0.143 14	0.013 65	0.588 28	0.8
H37	0.175 35	0.293 18	0.539 86	0.8
H38	0.097 92	0.350 66	0.603 70	0.8
H39	0.286 76	0.096 82	0.667 34	0.8
H40	0.344 07	0.571 76	0.697 47	0.8
H41	0.438 28	0.174 88	0.630 71	0.8
H42	0.440 27	0.644 59	0.563 41	0.8
H43	0.486 65	0.604 49	0.649 54	0.8
H44	0.347 51	0.727 63	0.617 99	0.8
H45	0.323 77	0.003 21	0.528 69	0.8
H46	0.280 54	0.599 34	0.499 69	0.8
H47	0.175 43	0.126 49	0.436 25	0.3058
H48	0.280 44	0.224 00	0.391 14	0.3058
H49	0.113 75	0.414 81	0.343 91	0.3058
H50	0.279 59	0.716 98	0.355 74	0.3058
H51	0.214 47	0.902 57	0.412 39	0.3058
H52	0.046 02	1.155 28	0.364 67	0.3058
H53	−0.089 96	0.656 34	0.351 34	0.3058
H54	0.008 18	0.388 16	0.424 33	0.3058
H55	−0.006 59	1.019 55	0.459 45	0.3058
H56	0.018 28	0.748 33	0.500 43	0.3058
H57	−0.040 53	1.239 73	0.264 15	0.0872
H58	−0.136 87	0.987 58	0.281 69	0.0872
H59	−0.030 80	0.451 25	0.251 82	0.0872
H60	−0.086 21	0.510 05	0.167 20	0.0872
H61	−0.166 19	0.607 24	0.227 45	0.0872
H62	0.076 11	1.112 15	0.181 28	0.0872
H63	0.043 06	0.669 42	−0.008 87	0.0472
H64	0.069 34	0.428 42	0.056 12	0.0472
H65	0.249 62	0.420 99	0.060 47	0.0472
H66	0.261 55	0.775 87	0.049 24	0.0472
H67	0.169 42	0.609 97	−0.077 31	0.0472
H68	0.261 91	0.338 45	−0.048 66	0.0472
H69	0.423 10	0.715 57	−0.018 24	0.0472
H70	0.332 11	0.929 91	−0.072 87	0.0472
H71	0.346 42	0.704 43	−0.158 48	0.0472
H72	0.394 17	0.400 88	−0.115 15	0.0472
H73	0.570 84	0.616 23	−0.068 10	0.0472
H74	0.525 81	0.924 58	−0.110 65	0.0472
H75	0.497 62	0.681 88	−0.209 02	0.0472
H76	0.554 00	0.385 64	−0.165 40	0.0472
H77	0.725 96	0.521 73	−0.152 46	0.0472
H78	0.694 60	0.864 00	−0.135 63	0.0472
H79	0.794 40	0.512 50	−0.284 60	0.0472

molecule refined to very large values, and were fixed at 0.80 Å^2. This molecule is pseudomonic acid A, which normally constitutes >90% of mupirocin; pseudomonic acids B and C are different in this end of the molecule, and these differences in co-crystallized impurities may explain the large displacement coefficients. The difference Fourier maps provided no indication of another conformation, and eliminating these atoms from the model did not result in their appearance in a difference Fourier map. Because the DFT calculation needs an ordered model, we choose to accept the very large displacement coefficients.

The root-mean-square deviation of the non-H atoms in the refined and optimized structures is 1.02 Å (Figure 3), suggesting that there are problems with the experimental structure (van de Streek and Neumann, 2014). The most notable differences are in the conformation of the nonyl chain and the interchange of the methyl group C1 and the hydroxyl group O16. There is a too-close intermolecular C1–O16 contact in the refined structure. We believe that the DFT structure is correct, as it results in a more reasonable geometry and hydrogen-bonding pattern. The discussion of the geometry uses the DFT-optimized structure. The asymmetric unit (with atom numbering) is illustrated in Figure 4, and the crystal structure is presented in Figure 5.

All of the bond distances fall within the normal ranges indicated by a Mercury Mogul Geometry Check (Macrae *et al.*, 2008). Only the C18–C13–C14 angle of 119.1° falls outside the normal range of 113(1)° (Z-score = 6.89). The C5–C4–C2–C1 torsion angle is flagged as unusual, but it lies in the tail of the normal distribution. The C5–C4–C6–C7 torsion lies within a very broad distribution, and the O8–C6–C4–C5 torsion lies in the tail of the normal *trans*/±*gauche* distribution. Only the O3–C2–C4–C5 torsion seems to be truly unusual (Figure 6).

https://doi.org/10.1017/S088571561600004X Published online by Cambridge University Press

TABLE II. DFT-optimized (CRYSTAL09) crystal structure of mupirocin Form I.

Crystal data	
$C_{26}H_{44}O_9$	$\beta = 100.9353°$
$M_r = 500.63$	$V = 1366.95$ Å^3
Monoclinic, $P2_1$	$Z = 2$
$a = 12.564\ 22$ Å	Synchrotron radiation, $\lambda = 0.413\ 685$ Å
$b = 5.103\ 56$ Å	$T = 295$ K
$c = 21.712\ 17$ Å	

Fractional atomic coordinates and isotropic displacement parameters (Å^2)

	x	y	Z	U_{iso}
C1	0.261 03	0.230 41	0.706 18	0.8
C2	0.318 76	0.396 43	0.664 30	0.8
O3	0.245 58	0.470 48	0.607 29	0.8
C4	0.417 07	0.252 47	0.647 26	0.8
C5	0.505 66	0.436 90	0.634 09	0.8
C6	0.382 16	0.055 97	0.594 90	0.8
C7	0.368 46	0.112 50	0.527 41	0.8
O8	0.463 56	−0.022 37	0.559 98	0.8
C9	0.298 14	−0.061 39	0.479 48	0.235
C10	0.214 49	0.067 12	0.427 51	0.235
C11	0.260 57	0.282 45	0.391 34	0.235
O12	0.181 81	0.355 53	0.337 73	0.235
C13	0.086 40	0.462 20	0.354 00	0.235
C14	0.029 15	0.248 96	0.385 85	0.235
C15	0.106 72	0.152 02	0.445 40	0.235
O16	−0.070 25	0.343 34	0.400 27	0.235
O17	0.113 11	0.363 71	0.488 99	0.235
C18	0.023 18	0.602 84	0.295 86	0.0671
C19	−0.004 00	0.444 23	0.236 28	0.0671
C20	−0.095 42	0.249 22	0.231 29	0.0671
C21	0.052 03	0.487 30	0.190 07	0.0671
C22	0.037 06	0.332 44	0.131 94	0.0671
O23	−0.030 46	0.159 96	0.116 72	0.0671
O24	0.110 20	0.399 39	0.096 26	0.0671
C25	0.107 49	0.236 95	0.041 56	0.0363
C26	0.211 17	0.272 57	0.016 52	0.0363
C27	0.207 46	0.099 05	−0.041 61	0.0363
C28	0.317 83	0.058 28	−0.060 17	0.0363
C29	0.362 79	0.304 37	−0.086 06	0.0363
C30	0.469 58	0.258 43	−0.108 35	0.0363
C31	0.504 16	0.497 89	−0.141 79	0.0363
C32	0.606 41	0.452 59	−0.168 60	0.0363
C33	0.630 94	0.679 20	−0.207 95	0.0363
O34	0.566 30	0.848 57	−0.230 38	0.0363
O35	0.733 01	0.673 82	−0.217 77	0.0363
H36	0.199 02	0.343 54	0.723 44	0.8
H37	0.318 18	0.159 29	0.747 22	0.8
H38	0.221 79	0.061 89	0.680 27	0.8
H39	0.349 60	0.575 38	0.689 73	0.8
H40	0.192 84	0.598 83	0.616 27	0.8
H41	0.452 62	0.137 25	0.688 71	0.8
H42	0.578 59	0.323 28	0.632 18	0.8
H43	0.525 58	0.580 49	0.671 86	0.8
H44	0.482 94	0.545 86	0.590 34	0.8
H45	0.334 77	−0.108 69	0.606 81	0.8
H46	0.385 28	0.309 42	0.512 75	0.8
H47	0.257 93	−0.208 88	0.503 72	0.3058
H48	0.355 03	−0.168 30	0.456 37	0.3058
H49	0.190 22	−0.087 61	0.392 73	0.3058
H50	0.330 00	0.210 38	0.373 24	0.3058
H51	0.285 81	0.454 29	0.420 49	0.3058
H52	0.109 89	0.613 69	0.389 79	0.3058
H53	0.007 98	0.083 71	0.354 01	0.3058
H54	0.069 52	−0.019 22	0.463 70	0.3058
H55	−0.052 15	0.443 13	0.438 92	0.3058
H56	0.167 41	0.340 25	0.527 11	0.3058
H57	0.073 17	0.770 24	0.287 65	0.0872
H58	−0.050 84	0.677 80	0.308 85	0.0872
H59	−0.070 93	0.054 95	0.218 16	0.0872
H60	−0.163 12	0.306 95	0.194 19	0.0872
H61	−0.125 25	0.239 58	0.275 19	0.0872
H62	0.114 60	0.636 79	0.195 80	0.0872
H63	0.036 73	0.289 87	0.006 72	0.0472
H64	0.097 70	0.033 04	0.054 91	0.0472
H65	0.280 60	0.218 83	0.053 09	0.0472
H66	0.221 41	0.479 05	0.005 21	0.0472
H67	0.151 02	0.186 21	−0.081 06	0.0472
H68	0.173 44	−0.092 82	−0.033 51	0.0472
H69	0.311 14	−0.096 80	−0.095 67	0.0472
H70	0.376 03	−0.014 21	−0.019 39	0.0472
H71	0.373 11	0.461 49	−0.050 99	0.0472
H72	0.302 21	0.376 66	−0.125 72	0.0472
H73	0.461 20	0.090 56	−0.140 44	0.0472
H74	0.533 71	0.205 16	−0.068 43	0.0472
H75	0.516 00	0.666 76	−0.110 01	0.0472
H76	0.438 19	0.552 71	−0.180 32	0.0472
H77	0.597 30	0.277 62	−0.198 60	0.0472
H78	0.677 69	0.414 83	−0.132 02	0.0472
H79	0.741 71	0.819 49	−0.245 27	0.0472

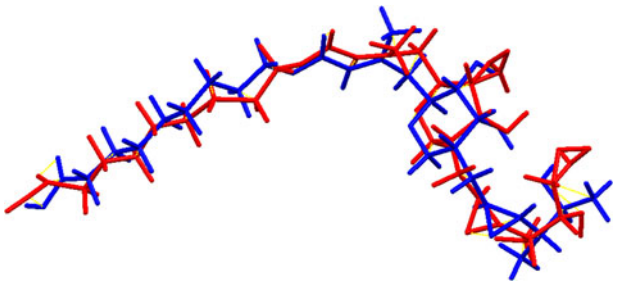

Figure 3. (Color online) Comparison of the refined and optimized structures of mupirocin. The Rietveld refined structure is colored red, and the DFT-optimized structure is blue.

A quantum mechanical conformational examination (DFT/B3LYP functional/6-31G* basis set/water) using Spartan '14 indicated that the observed conformation is ∼6 kcal mole^{-1} higher in energy than a local minimum. A molecular mechanics (MMFF) sampling of conformational space indicated that the observed solid-state conformation is 48.4 kcal mole^{-1} higher in energy than the minimum energy conformation, which has the carboxylic acid end of the nonyl chain curled back toward the rest of the molecule. The energy difference indicates that van der Waals forces contribute significantly to the crystal energy.

An analysis of the contributions to the total crystal energy using the Forcite module of Materials Studio (Accelrys, 2013) suggests that the crystal energy is dominated by angle deformation contributions. The intermolecular energy appears to be dominated by van der Waals and electrostatic contributions, which in this force-field-based analysis include hydrogen bonds. The hydrogen bonds are better analyzed using the results of the DFT calculation.

As expected, the three hydroxyl groups O17–H56, O16–H55, and O3–H40, as well as the carboxylic acid hydrogen H79, participate in hydrogen bonds (Table III). The hydroxyl

https://doi.org/10.1017/S088571561600004X Published online by Cambridge University Press

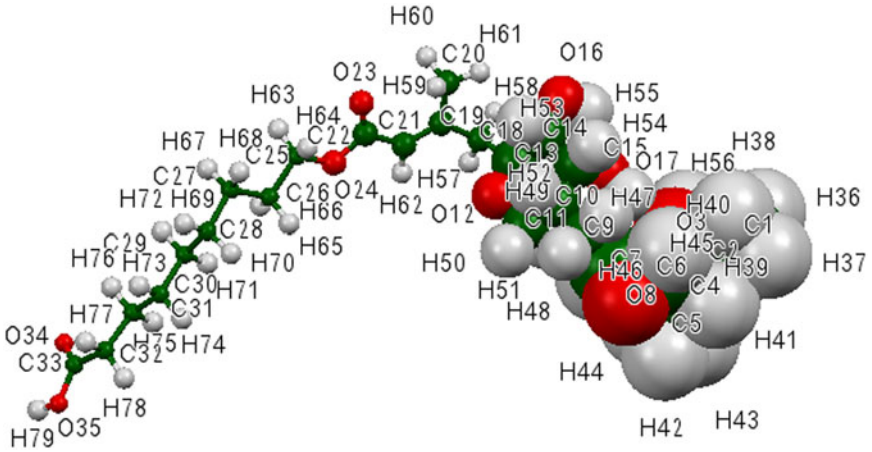

Figure 4. (Color online) The molecular structure of mupirocin, with the atom numbering. The atoms are represented by 50% probability spheroids.

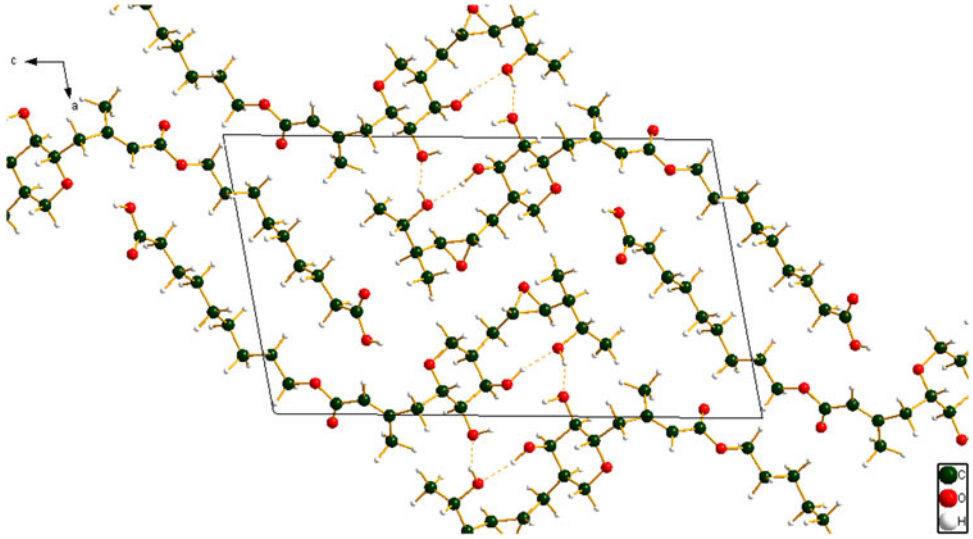

Figure 5. (Color online) The crystal structure of mupirocin Form I, viewed down the *b*-axis. The hydrogen bonds are shown as dashed lines.

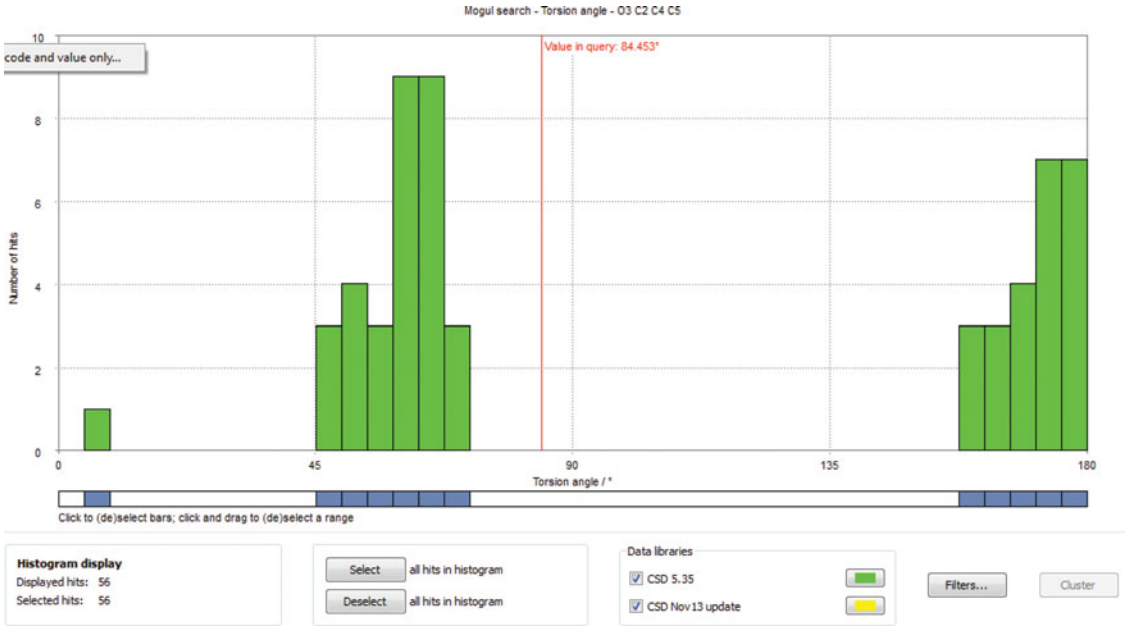

Figure 6. (Color online) The O3–C2–C4–C5 torsion angle compared to the distribution of similar torsions in the CSD. Although the value of 84.4° is closer to a *gauche* conformation, it is unusual.

https://doi.org/10.1017/S088571561600004X Published online by Cambridge University Press

TABLE III. Hydrogen bonds in the DFT-optimized structure of mupirocin Form I.

D–H···A	D–H (Å)	H···A (Å)	D···A (Å)	D–H···A(°)	Overlap (*e*)	Energy, (kcal mol^{-1})
O17–H56···O3	0.975	1.946	2.836	150.5	0.050	12.2
O3–H40···O16	0.977	1.962	2.892	158.2	0.042	11.2
O16–H55···O17	0.971	1.949	2.710	112.1	0.018	7.3
O35–H79···O12	0.973	2.392	3.138	133.2	0.021	7.9
C32–H77···O34	1.099	2.307	3.362	160.4	0.020	

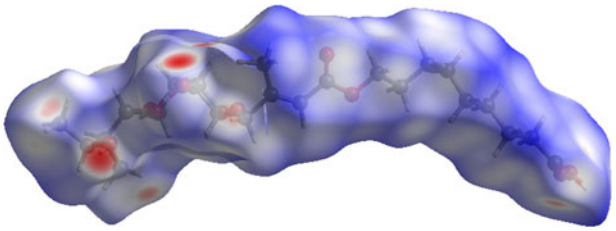

Figure 7. (Color online) The Hirshfeld surface of mupirocin. Intermolecular contacts longer than the sums of the van der Waals radii are colored blue, and contacts shorter than the sums of the radii are colored red. Contacts equal to the sums of the radii are white.

group O17–H56 makes an intramolecular hydrogen bond to the hydroxyl oxygen O3, with a graph set *S1,1*(10) (Etter, 1990; Bernstein *et al.*, 1995; Shields *et al.*, 2000). This hydrogen bond is fairly strong (Rammohan and Kaduk, 2015, unpublished results). The hydroxyl group O16–H55 makes a weaker intramolecular hydrogen bond to O17, with graph set *S*1,1(5). The hydroxyl group O3–H40 makes a hydrogen bond to hydroxyl oxygen O16, with graph set *C*1,1(11). The result is a helical hydrogen bond chain parallel to the *b*-axis. The carboxylic acid makes a fairly weak hydrogen bond to the ether oxygen O12. An additional weak intermolecular C–H···O hydrogen bond also contributes to the crystal packing. The resulting hydrogen bond network is three-dimensional.

The volume of the Hirshfeld surface (Figure 7; Hirshfeld, 1977; McKinnon *et al.*, 2004; Spackman and Jayatilaka, 2009; Wolff *et al.*, 2012) is 672.78 Å^3, 98.44% of half the unit-cell volume. The molecules are thus not tightly packed. The only significant close contacts (red in Figure 7) involve the hydrogen bonds.

The Bravais–Friedel–Donnay–Harker (Bravais, 1866; Friedel, 1907; Donnay and Harker, 1937) morphology suggests that we might expect a needle-like morphology for mupirocin Form I, with ⟨010⟩ as the long axis. A tenth-order spherical harmonic preferred orientation model was included in the refinement; the texture index was 1.214, indicating that preferred orientation was significant in this rotated capillary specimen.

The powder pattern of mupirocin Form I has been submitted to ICDD for inclusion in the PDF. The pattern was based on a Le Bail fit to the pattern, so it is independent of any imperfection in the structural model.

SUPPLEMENTARY MATERIAL

To view supplementary material for this article, please visit http://dx.doi.org/10.1017/S088571561600004X

ACKNOWLEDGEMENTS

The use of the Advanced Photon Source at Argonne National Laboratory was supported by the U. S. Department of Energy, Office of Science, Office of Basic Energy Sciences, under Contract No. DE-AC02-06CH11357. This work was partially supported by the International Centre for Diffraction Data. We thank Lynn Ribaud for his assistance in data collection.

Accelrys (**2013**). *Materials Studio 7.0* (Accelrys Software Inc., San Diego, CA).

Allen, F. H. (**2002**). "The Cambridge Structural Database: a quarter of a million crystal structures and rising," Acta Crystallogr., B: Struct. Sci. **58**, 380–388.

Altomare, A., Cuocci, C., Giacovazzo, C., Moliterni, A., Rizzi, R., Corriero, N., and Falcicchio, A. (**2013**). "EXPO2013: a kit of tools for phasing crystal structures from powder data", J. Appl. Crystallogr. **46**, 1231–1235.

Bernstein, J., Davis, R. E., Shimoni, L., and Chang, N. L. (**1995**). "Patterns in hydrogen bonding: functionality and graph set analysis in crystals," Angew. Chem. Int. Ed. Engl. **34**(15), 1555–1573.

Bravais, A. (**1866**). *Etudes Cristallographiques* (Gauthier Villars, Paris).

Bruno, I. J., Cole, J. C., Kessler, M., Luo, J., Motherwell, W. D. S., Purkis, L. H., Smith, B. R., Taylor, R., Cooper, R. I., Harris, S. E., and Orpen, A. G. (**2004**). "Retrieval of crystallographically-derived molecular geometry information," J. Chem. Inf. Sci. **44**, 2133–2144.

David, W. I. F., Shankland, K., van de Streek, J., Pidcock, E., Motherwell, W. D. S., and Cole, J. C. (**2006**). "DASH: a program for crystal structure determination from powder diffraction data," J. Appl. Crystallogr. **39**, 910–915.

Donnay, J. D. H. and Harker, D. (**1937**). "A new law of crystal morphology extending the law of Bravais," Am. Mineral. **22**, 446–467.

Dovesi, R., Orlando, R., Civalleri, B., Roetti, C., Saunders, V. R., and Zicovich-Wilson, C. M. (**2005**). "CRYSTAL: a computational tool for the *ab initio* study of the electronic properties of crystals," Z. Kristallogr. **220**, 571–573.

Etter, M. C. (**1990**). "Encoding and decoding hydrogen-bond patterns of organic compounds," Acc. Chem. Res. **23**(4), 120–126.

Finger, L. W., Cox, D. E., and Jephcoat, A. P. (**1994**). "A correction for powder diffraction peak asymmetry due to axial divergence," J. Appl. Crystallogr. **27**(6), 892–900.

Friedel, G. (**1907**). "Etudes sur la loi de Bravais," Bull. Soc. Fr. Mineral. **30**, 326–455.

Fuller, A. T., Mellows, G., Woolford, M., Banks, G. T., Barrow, K. D., and Chain, E. B. (**1971**). "Pseudomonic acid: an antibiotic produced by Pseudomonas fluorescens," Nature **234**, 416–417.

Gatti, C., Saunders, V. R., and Roetti, C. (**1994**). "Crystal-field effects on the topological properties of the electron-density in molecular crystals - the case of urea," J. Chem. Phys. **101**, 10686–10696.

Greenway, M. J., Salt, S. D., Valder, C. E., and Curzons, A. D. (**1997**). "Polymorphs of Crystalline Mupirocin," U.S. Patent 5,594,026.

Hirshfeld, F. L. (**1977**). "Bonded-atom fragments for describing molecular charge densities," Theor. Chem. Acta **44**, 129–138.

ICDD (**2014**), PDF-4+ 2014 (Database) edited by Dr. Soorya Kabekkodu, International Centre for Diffraction Data, Newtown Square, PA, USA.

Larson, A. C. and Von Dreele, R. B. (**2004**). *General Structure Analysis System (GSAS)* (Report LAUR 86-784) Los Alamos National Laboratory.

Lee, P. L., Shu, D., Ramanathan, M., Preissner, C., Wang, J., Beno, M. A., Von Dreele, R. B., Ribaud, L., Kurtz, C., Antao, S. M., Jiao, X., and Toby, B. H. (**2008**). "A twelve-analyzer detector system for high-resolution powder diffraction," J. Synchrotron Radiat. **15**(5), 427–432.

Louër, D. and Boultif, A. (**2007**). "Powder pattern indexing and the dichotomy algorithm," Z. Kristallogr. Suppl.," 2007, 191–196.

Macrae, C. F., Bruno, I. J., Chisholm, J. A., Edington, P. R., McCabe, P., Pidcock, E., Rodriguez-Monge, L., Taylor, R., van de Streek, J., and Wood, P. A. (**2008**). "Mercury CSD 2.0 – new features for the visualization and investigation of crystal structures," J. Appl. Crystallogr. **41**, 466–470.

McKinnon, J. J., Spackman, M. A., and Mitchell, A. S. (**2004**). "Novel tools for visualizing and exploring intermolecular interactions in molecular crystals," Acta Crystallogr., B **60**, 627–668.

Shields, G. P., Raithby, P. R., Allen, F. H., and Motherwell, W. S. (**2000**). "The assignment and validation of metal oxidation states in the Cambridge Structural Database," Acta Crystallogr. B, Struct. Sci. **56**(3), 455–465.

Spackman, M. A., and Jayatilaka, D. (**2009**). "Hirshfeld surface analysis," CrystEngComm **11**, 19–32.

Stephens, P. W. (**1999**). "Phenomenological model of anisotropic peak broadening in powder diffraction," J. Appl. Crystallogr. **32**, 281–289.

Sutherland, R., Boon, R. J., Griffin, K. E., Masters, P. J., Slocombe, B., and White, A. R. (**1985**). "Antibacterial activity of mupirocin (pseudomonic acid), a new antibiotic for topical use," Antimicrob. Agents Chemother. **27**(4), 495–498.

Sykes, R. A., McCabe, P., Allen, F. H., Battle, G. M., Bruno, I. J., and Wood, P. A. (**2011**). "New software for statistical analysis of Cambridge Structural Database data," J. Appl. Crystallogr. **44**, 882–886.

Thompson, P., Cox, D. E., and Hastings, J. B. (**1987**). "Rietveld refinement of Debye-Scherrer synchrotron X-ray data from Al_2O_3," J. Appl. Crystallogr. **20**(2), 79–83.

van de Streek, J., and Neumann, M. A. (**2014**). "Validation of molecular crystal structures from powder diffraction data with dispersion-corrected density functional theory (DFT-D)," Acta Crystallogr., B, Struct. Sci., Crystal Eng. Mater. **70**(6), 1020–1032.

Wang, J., Toby, B. H., Lee, P. L., Ribaud, L., Antao, S. M., Kurtz, C., Ramanathan, M., Von Dreele, R. B., and Beno, M. A. (**2008**). "A dedicated powder diffraction beamline at the Advanced Photon Source: Commissioning and early operational results," Rev. Sci. Instrum. **79**, 085105.

Wavefunction, Inc. (**2013**). Spartan '14 Version 1.1.0, Wavefunction Inc., 18401 Von Karman Ave., Suite 370, Irvine CA 92612.

Wolff, S. K., Grimwood, D. J., McKinnon, M. J., Turner, M. J., Jayatilaka, D., and Spackman, M. A. (**2012**). *Crystal Explorer Version 3.1* (University of Western Australia, Perth, Western Australia).

https://doi.org/10.1017/S088571561600004X Published online by Cambridge University Press